$(PPh_3)_3RhCNB(CF_3)_3$ and $(PPh_3)_3RhNCB(CF_3)_3$: Isocyano- and Cyanoborate Complexes of Tris(triphenylphosphine)rhodium(I)

Maik Finze,*[,†,‡] Eduard Bernhardt,[†] Helge Willner,*[,†] and Christian W. Lehmann*[,§]

FB C-Anorganische Chemie, Bergische Universität Wuppertal, Gaussstrasse 20, D-42097 Wuppertal, Germany

Received February 13, 2006

The reactions of $K[(CF_3)_3BNC]$ and $K[(CF_3)_3BCN]$ with $(PPh_3)_3RhCl$ in ethanol resulted in the rhodium(I) complexes $(PPh_3)_3RhNCB(CF_3)_3$ and $(PPh_3)_3RhCNB(CF_3)_3$, respectively. Their ^{15}N-labeled isotopomers were synthesized from the corresponding borate anions. The complexes were characterized by UV, Raman, and multi-NMR spectroscopy, and the crystal structures were obtained. The spectroscopic and structural data are compared to those of the potassium borates and to related rhodium(I) complexes.

Introduction

Since the discovery of Wilkinsons catalyst, chlorotris(triphenylphosphine)rhodium(I), $(PPh_3)_3RhCl$, in 1964,[1] numerous applications in catalytic processes have been developed such as hydrogenations and hydroformulations.[2] Many derivatives of $(PPh_3)_3RhCl$ have been synthesized, and their chemistry has been investigated, especially their catalytic properties.[2,3] In addition, the chloro ligand was replaced by cyano,[4] $NCBPh_3$, $CNBPh_3$,[5−8] NCMe,[9,10] and many other groups.

Recently we reported the two-step synthesis of the isocyanotris(trifluoromethyl)borate anion, $[(CF_3)_3BNC]^-$,[11] using the borane carbonyl $(CF_3)_3BCO$[12,13] as starting material according to eq 1.

$$(CF_3)_3BCO \xrightarrow[-80\ ^\circ C \rightarrow RT,\ CH_2Cl_2]{+\ HCN,\ -\ CO} (CF_3)_3BNCH \xrightarrow[-20\ ^\circ C \rightarrow RT,\ toluene]{+Li[N(SiMe_3)_2],\ -HN(SiMe_3)_2} Li[(CF_3)_3BNC] \quad (1)$$

The isocyanoborate anion is indefinitely stable at room temperature, and heating above 100 °C causes isomerization to the cyanoborate anion according to eq 2.

$$K[(CF_3)_3BNC] \xrightarrow{\Delta} K[(CF_3)_3BNC] \quad (2)$$

The isomerization enthalpy $\Delta H_{iso} = -35 \pm 4$ kJ mol^{-1} and the activation energy $E_a = 180 \pm 20$ kJ mol^{-1} of this process were determined.[11] Since both anions are readily available, they can be used as ligands in coordination chemistry. Here we report the syntheses of $(PPh_3)_3RhCNB(CF_3)_3$, $(PPh_3)_3RhNCB(CF_3)_3$, and their ^{15}N isotopomers as well as their thermal, spectroscopic, and structural properties. The data are compared to those of $K[(CF_3)_3BCN]$ and $K[(CF_3)_3BNC]$ as well as the related rhodium(I) complexes $(PPh_3)_3RhCN$,[4] $(PPh_3)_3RhCNBPh_3$,[5−8] $[(PPh_3)_3RhCNMe]^+$,[9,10] and $(PPh_3)_3RhNCBPh_3$.[5−8]

Results and Discussion

Syntheses. Treatment of $(PPh_3)_3RhCl$ with either $K[(CF_3)_3BNC]$ or $K[(CF_3)_3BCN]$[11] in ethanol at room temperature yields the distorted square planar Rh(I) complex $(PPh_3)_3RhCNB(CF_3)_3$ or $(PPh_3)_3RhNCB(CF_3)_3$, respectively (eq 3).

$$(PPh_3)_3RhCl + K[(CF_3)_3BX] \xrightarrow[RT,\ EtOH]{90\%} (PPh_3)_3RhXB(CF_3)_3 + KCl \quad (X = NC,CN) \quad (3)$$

After removal of the solvent the complexes are isolated from the reaction mixture by extraction with dichloromethane. In an analogous manner $(PPh_3)_3RhNCBPh_3$[5] was prepared. However, the isomer $(PPh_3)_3RhCNBPh_3$ was obtained by addition of the Lewis acid Ph_3B to $(PPh_3)_3RhCN$; a metathesis reaction employing a $[Ph_3BNC]^-$ salt was not feasible, because it is unknown, so far.[5] $(PPh_3)_3RhCN$ is obtained by ligand exchange from $(PPh_3)_3RhCl$ and KCN,[4] while the isoelectronic complex $(PPh_3)_3RhNC$ is unknown, probably due to a low isomerization barrier from the isocyano to the thermodynamically more stable cyano derivative.

Attempts to isomerize $(PPh_3)_3RhNCB(CF_3)_3$ to $(PPh_3)_3RhCNB(CF_3)_3$ by heating failed, due to the strong C−B bond resulting from the high Lewis acidity of $B(CF_3)_3$. This is in contrast to the properties of $(PPh_3)_3RhNCBPh_3$,[5] which easily isomerizes. Both $(PPh_3)_3RhNCB(CF_3)_3$ and $(PPh_3)_3RhCNB$-

* To whom correspondence should be addressed. M.F.: Tel: (+49) 211-81-13144. E-mail: maik.finze@uni-duesseldorf.de. H.W.: Tel: (+49) 202-439-2517. Fax: (+49) 202-439-3053. E-mail: willner@uni-wuppertal.de. C.W.L.: Tel: (+49) 208-306-2989. E-mail: lehmann@mpi-muelheim.mpg.de.

† Bergische Universität Wuppertal.

§ Max-Planck-Institut für Kohlenforschung.

‡ Present address: Institut für Anorganische Chemie und Strukturchemie II, Heinrich-Heine-Universität Düsseldorf, Universitätsstr. 1, D-40225 Düsseldorf, Germany.

(1) Jardine, F. H.; Osborn, J. A.; Wilkinson, G.; Young, J. F. *Chem. Ind. (London)* **1965**, 560.

(2) Jardine, F. H. *Prog. Inorg. Chem.* **1981**, *28*, 63.

(3) Wilkinson, G.; Cotton, F. A. *Advanced Inorganic Chemistry*, 6th ed.; John Wiley & Sons: New York, 1999.

(4) Favero, G.; Rigo, P. *Gazz. Chim. Ital.* **1972**, *102*, 597.

(5) Carlton, L.; Weber, R. *Inorg. Chem.* **1996**, *35*, 5843.

(6) Carlton, L.; Weber, R.; Levendis, D. C. *Inorg. Chem.* **1998**, *37*, 1264.

(7) Cîrcu, V.; Fernandes, M. A.; Carlton, L. *Polyhedron* **2002**, *21*, 1775.

(8) Fernandes, M. A.; Cîrcu, V.; Weber, R.; Varnali, T.; Carlton, L. *J. Chem. Crystallogr.* **2002**, *32*, 273.

(9) Clegg, W.; Garner, C. D.; Heyworth, S. *Acta Crystallogr., Sect. C: Cryst. Struct. Commun.* **1989**, *C45*, 1996.

(10) Pimblett, G.; Garner, C. D.; Clegg, W. *J. Chem. Soc., Dalton Trans.* **1985**, 1977.

(11) Finze, M.; Bernhardt, E.; Lehmann, C. W.; Willner, H. *J. Am. Chem. Soc.* **2005**, *127*, 10712.

(12) Terheiden, A.; Bernhardt, E.; Willner, H.; Aubke, F. *Angew. Chem., Int. Ed.* **2002**, *41*, 799.

(13) Finze, M.; Bernhardt, E.; Terheiden, A.; Berkei, M.; Willner, H.; Christen, D.; Oberhammer, H.; Aubke, F. *J. Am. Chem. Soc.* **2002**, *124*, 15385.

10.1021/om060135z CCC: $33.50
Publication on Web 04/28/2006

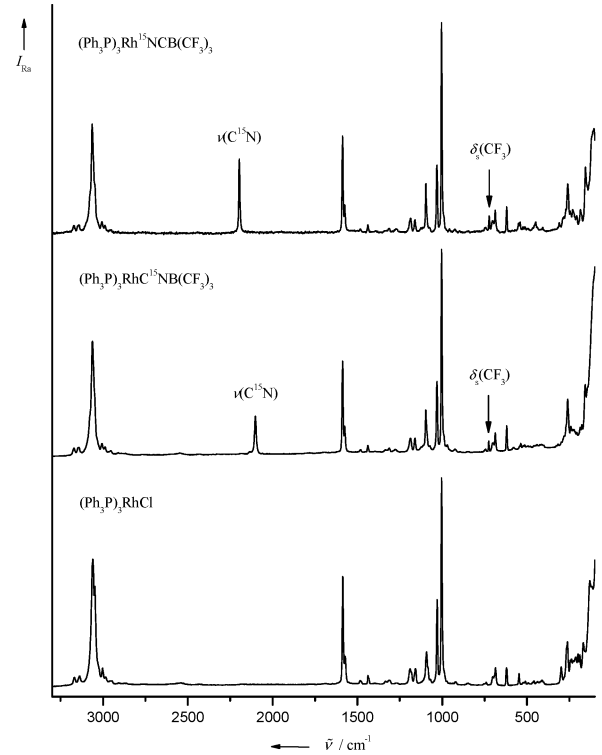

Figure 1. Raman spectra of $(PPh_3)_3Rh^{15}NCB(CF_3)_3$, $(PPh_3)_3RhC^{15}NB(CF_3)_3$, and $(PPh_3)_3RhCl$.

Table 1. Comparison of ν(CN) in Selected Rh(I) Complexes and Their Corresponding Ligands[a]

complex	$\nu(CN)_{complex}$[b]	ref	salt	$\nu(CN)_{ligand}$[b]	ref
$(PPh_3)_3RhNCB(CF_3)_3$	2227 (2196)	*c*	$K[(CF_3)_3BCN]$	2244 (2216)	*c*
$(PPh_3)_3RhCNB(CF_3)_3$	2136 (2101)	*c*	$K[(CF_3)_3BNC]$	2169 (2132)	*c*
$(PPh_3)_3RhNCBPh_3$	2184 (2154)	5	$K[Ph_3BCN]$	2180	8
$(PPh_3)_3RhCNBPh_3$	2144 (2110)	5		n.o.[d]	
$(PPh_3)_3RhCN$	2085	4	KCN[e]	2076	14

[a] Wavenumbers in cm^{-1}. [b] Values in parentheses: $\nu(C^{15}N)$. [c] This work. [d] n.o. = not observed. [e] Dissolved in H_2O.

$(CF_3)_3$ decompose exothermically at 140 °C according to DSC measurements.

Raman Spectroscopy. The Raman spectra of $(PPh_3)_3RhC^{15}NB(CF_3)_3$ and $(PPh_3)_3Rh^{15}NCB(CF_3)_3$ are dominated by the spectrum of the $(PPh_3)_3Rh$ moiety, as shown in Figure 1. The CN stretching band in both rhodium complexes is shifted to lower wavenumbers in comparison to that of the potassium borates (Table 1),[11] indicating significant M→CN and M→NC π-back-bonding.[15,16] The higher ν(CN) shift of −33 cm^{-1} in $(PPh_3)_3RhCNB(CF_3)_3$ compared to −17 cm^{-1} in $(PPh_3)_3RhNCB(CF_3)_3$ is due to the enhanced π-acceptor ability of isocyanides compared to their cyano isomers.[15−17]

In agreement with the higher Lewis acidity of $(CF_3)_3B$ compared to Ph_3B, ν(CN) of $K[(CF_3)_3BCN]$ and $(PPh_3)_3RhNCB(CF_3)_3$ are observed at higher wavenumbers than ν(CN) of $K[Ph_3BCN]$[18] and $(PPh_3)_3RhNCBPh_3$,[5] respectively. In contrast, for $(PPh_3)_3RhCNBPh_3$[5] a higher ν(CN) value in comparison to $(PPh_3)_3RhCNB(CF_3)_3$ was found. Since salts of the $[Ph_3BNC]^-$ anion are unknown, no comparison to $K[(CF_3)_3BNC]$ is possible. The $[(CF_3)_3BNC]^-$ ligand seems to be a stronger π-acceptor and weaker σ-donor than $[Ph_3BNC]^-$. Also for the anions $[(CF_3)_3BCN]^-$ and $[Ph_3BCN]^-$ a similar trend is found: the difference in ν(CN) is reduced from the potassium salts (64 cm^{-1}) to the Rh(I) complexes (43 cm^{-1}).

Table 2. Experimental Bond Parameters[a] of the $(CF_3)_3B$ Fragments in $(PPh_3)_3RhNCB(CF_3)_3$, $(PPh_3)_3RhCNB(CF_3)_3$, $[(CF_3)_3BCN]^-$, and $[(CF_3)_3BNC]^-$

parameter	$(PPh_3)_3RhNCB(CF_3)_3$	$[(CF_3)_3BCN]^-$[b 11]	$(PPh_3)_3RhCNB(CF_3)_3$	$[(CF_3)_3BNC]^-$[b 11]
bond lengths [Å]				
C−N	1.139(4)	1.147(3)	1.151(3)	1.154(2)
B−C/B−N	1.597(4)	1.589(3)	1.526(3)	1.514(2)
$B-CF_3$[a]	1.610(5)	1.626(2)	1.627(4)	1.625(2)
C−F[a]	1.348(6)	1.356(2)	1.354(4)	1.353(2)
bond angles [deg]				
B−C−N/B−N−C	173.8(3)	179.4(2)	178.0(2)	179.84(18)
CF_3-B-CN/CF_3-B-NC[a]	108.5(3)	108.7(1)	108.7(2)	108.7(1)
CF_3-B-CF_3[a]	110.4(3)	110.3(1)	110.2(2)	110.3(1)
F−C−F[a]	104.9(4)	105.1(1)	105.2(2)	105.1(1)

[a] Mean values. [b] K^+ salt.

Also for the anions $[(CF_3)_3BCN]^-$ and $[Ph_3BCN]^-$ a similar trend is found: the difference in ν(CN) is reduced from the potassium salts (64 cm^{-1}) to the Rh(I) complexes (43 cm^{-1}).

Solid-State Structures of $(PPh_3)_3RhNCB(CF_3)_3$ and $(PPh_3)_3RhCNB(CF_3)_3$. The most relevant bond parameters of $(PPh_3)_3RhNCB(CF_3)_3 \cdot 1.5CH_2Cl_2$ and $(PPh_3)_3RhCNB(CF_3)_3$ obtained from X-ray crystal structure analysis are compared to the corresponding values of $K[(CF_3)_3BCN]$ and $K[(CF_3)_3BNC]$ in Table 2 and of related Rh(I) complexes in Table 3, respectively. In Figure 2 the molecular structures of $(PPh_3)_3RhNCB(CF_3)_3$ and $(PPh_3)_3RhCNB(CF_3)_3$ in the solid state are depicted.

The Rh(I) complexes crystallize in the monoclinic space group $P2_1/c$ and $P2_1/n$, respectively, and possess C_1 symmetry. In contrast to $(PPh_3)_3RhCNB(CF_3)_3$, $(PPh_3)_3RhNCB(CF_3)_3$ crystallizes as a solvate with 1.5 molecules of dichloromethane per formula unit, which are disordered. The arrangements of both complexes in their crystals are similar; they are stacked along the *a* axis and form layers in the *b*,*c* plane.

The shorter C−N bond lengths in the Rh(I) complexes compared to the respective potassium borates (Table 2) are not significant ($<3\sigma$). They are furthermore in contrast to the lower wavenumbers of the CN stretching bands in the metal complexes, which indicate weaker and hence elongated C−N bonds. The coordination of the borate anions to the Rh atom has only small effects on the bond parameters of the $(CF_3)_3B-X$ fragments (X = C, N).

A comparison of the C−N bond lengths of the Rh(I)−CN and Rh(I)−NC complexes listed in Table 3 is somewhat arbitrary, because the differences are small and not significant. More information is obtained by comparison of the bond lengths of Rh−P(2) in *trans* position to the cyano/isocyano ligand. The stronger *trans* effect of Rh−C over Rh−N is evident in a longer Rh−P(2) bond (Table 3). Furthermore within both series Rh−CN and Rh−NC, a significant decrease of d(Rh−P(2)) is accompanied by a decrease in Lewis acidity of the other group bonded to the C≡N system. Hence, $[(CF_3)_3BCN]^-$ and $[(CF_3)_3BNC]^-$ are more strongly bonded to rhodium than $[Ph_3BNC]^-$ and $[Ph_3BCN]^-$, respectively. This observation is in agreement with the vibrational data: $[(CF_3)_3BNC]^-$ and $[(CF_3)_3BCN]^-$ are stronger π-acceptors than the triphenylborate anions.

UV Spectroscopy. The UV−vis spectra of $(PPh_3)_3RhCNB(CF_3)_3$ and $(PPh_3)_3RhNCB(CF_3)_3$ presented in Figure 3 are similar. A strong broad absorption is observed between approximately 650 and 250 nm. In the spectral range from 650 to

(14) Siebert, H. *Anwendungen der Schwingungsspektroskopie in der Anorganischen Chemie*; Springer-Verlag: Heidelberg, 1966.
(15) Treichel, P. M. *Adv. Organomet. Chem.* **1973**, *11*, 21.
(16) Singleton, E.; Oosthuizen, H. E. *Adv. Organomet. Chem.* **1983**, *22*, 209.
(17) Kuznetsov, M. L.; Pombeiro, A. J. L. *J. Chem. Soc., Dalton Trans.* **2003**, 738.
(18) Brehm, E.; Haag, A.; Hesse, G. *Liebigs Ann. Chem.* **1970**, *737*, 80.

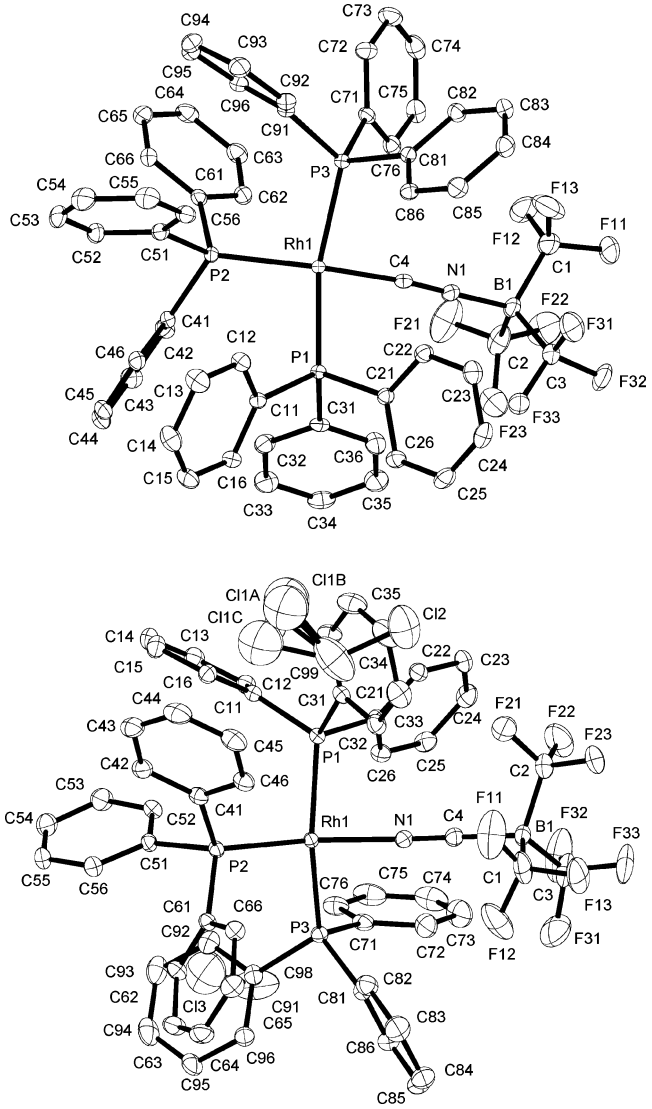

Figure 2. Formula units of $(PPh_3)_3RhCNB(CF_3)_3$ (top) and $(PPh_3)_3RhNCB(CF_3)_3 \cdot 1.5CH_2Cl_2$ (bottom) in their crystal structures (50% probability ellipsoids).

500 nm, absorption of $(PPh_3)_3RhCNB(CF_3)_3$ is stronger compared to its isomer in accordance with its more intense color: $(PPh_3)_3RhCNB(CF_3)_3$ is red, whereas $(PPh_3)_3RhNCB(CF_3)_3$ is orange. The absorptions are probably due to $\pi \rightarrow \pi^*$ transitions in the phenyl groups and transitions with participation of the d

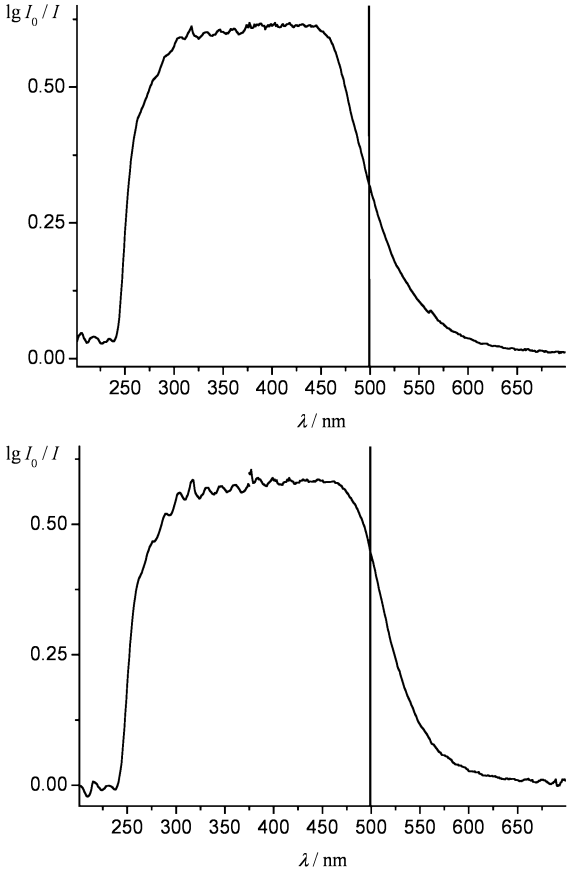

Figure 3. UV spectra of $(PPh_3)_3RhNCB(CF_3)_3$ (top) and $(PPh_3)_3RhCNB(CF_3)_3$ (bottom).

orbitals of rhodium, deduced from $\epsilon_{max} = 125-140$ L mol^{-1} cm^{-1}. The $\pi \rightarrow \pi^*$ transitions explain the vibrational progressions in the excited state with spacings of about 1450 cm^{-1}.

In contrast to the UV−vis spectra of $(PPh_3)_3RhCNB(CF_3)_3$ and $(PPh_3)_3RhNCB(CF_3)_3$, the spectrum of $(PPh_3)_3RhCl$ is dominated by strong charge transfer bands due to the more redox-sensitive chloro ligand ($\epsilon_{max} = 1500$ L mol^{-1} cm^{-1}).[19,20]

NMR Spectroscopy. The NMR spectroscopic data of $(PPh_3)_3RhCNB(CF_3)_3$ and $(PPh_3)_3RhNCB(CF_3)_3$ as well as some related compounds are collected in Table 4.

The $^{31}P\{^1H\}$ NMR spectra of $(PPh_3)_3Rh^{14}NCB(CF_3)_3$ and $(PPh_3)_3Rh^{15}NCB(CF_3)_3$ in Figure 4 show signals at 44.2 ppm with a relative intensity of one for the *trans* P atom and at 30.6

Table 3. Selected Bond Parameters of $(PPh_3)_3RhCNB(CF_3)_3$, $(PPh_3)_3RhNCB(CF_3)_3$, and Related Rhodium(I) Complexes

parameter	$(PPh_3)_3Rh$-$NCB(CF_3)_3$	$(PPh_3)_3Rh$-$CNB(CF_3)_3$	$(PPh_3)_3Rh$-$NCBPh_3$	$(PPh_3)_3RhCN$-BPh_3	$[(PPh_3)_3Rh$-NCMe$][BPh_4]$	$[(PPh_3)_3Rh$-NCMe$][BF_4]$	$(PPh_3)_3Rh$-CN
bond lengths [Å]							
C−N	1.139(4)	1.151(3)	1.143(3)	1.140(3)	1.130(6)	1.134(17)	1.121(4)
Rh−N/Rh−C	2.067(2)	1.957(2)	2.070(2)	2.005(2)	2.045(3)	2.015(10)	2.017(3)
C−B/N−B/C−C	1.597(4)	1.526(3)	1.637(4)	1.604(3)	1.456(9)	1.516(23)	
Rh−P(2)	2.2501(7)	2.3481(5)	2.2484(7)	2.3180(7)	2.262(1)	2.261(3)	2.3146(8)
Rh−P(1)	2.3240(7)	2.3218(5)	2.3112(8)	2.3048(7)	2.361(1)	2.311(3)	2.3433(8)
Rh−P(3)	2.3221(7)	2.3597(5)	2.3227(7)	2.3229(6)	2.315(1)	2.367(3)	2.2972(8)
bond angles [deg]							
Rh−N−C/Rh−C−N/Rh−C−C	169.8(2)	171.27(19)	172.1(2)	173.7(2)	171.8(3)	169.5(11)	171.0(3)
N−C−B/C−N−B/N−C−C	173.8(3)	178.0(2)	178.1(2)	177.4(2)	178.3(5)	177.2(14)	
N−Rh−P(2)/C−Rh−P(2)	157.96(7)	157.65(6)	166.78(6)	165.56(6)	169.6(1)	175.2(3)	159.25(9)
N−Rh−P(1)/C−Rh−P(1)	85.96(7)	84.26(6)	83.11(5)	83.03(6)	82.3(1)	87.7(3)	84.95(9)
N−Rh−P(3)/C−Rh−P(3)	86.58(7)	88.47(6)	84.85(6)	84.80(6)	87.3(1)	83.6(3)	85.31(9)
P(1)−Rh−P(2)	98.36(3)	97.656(18)	101.12(2)	101.32(2)	95.0(1)	94.9(1)	98.01(3)
P(1)−Rh−P(3)	153.73(3)	158.896(19)	157.99(2)	157.52(2)	167.1(1)	170.3(1)	155.82(3)
P(2)−Rh−P(3)	97.97(3)	96.594(18)	94.76(2)	95.13(2)	96.4(1)	94.1(1)	98.91(3)
ref	*a*	*a*	8	8	9	10	8

Table 4. NMR Spectroscopic Data of $(PPh_3)_3RhNCB(CF_3)_3$, $(PPh_3)_3RhCNB(CF_3)_3$, and Related Species[a]

parameter	$[(CF_3)_3BCN]^-$	$[(CF_3)_3BNC]^-$	$(PPh_3)_3Rh$-$NCB(CF_3)_3$	$(PPh_3)_3Rh$-$CNB(CF_3)_3$	$(PPh_3)_3Rh$-$NCBPh_3$	$(PPh_3)_3Rh$-$CNBPh_3$	$[(PPh_3)_3Rh$-$NCMe]^{+b}$	$(PPh_3)_3Rh$-CN
$\delta(^{11}B)$	−22.3	−17.5	−22.2	−17.0	n.o.[c]	n.o.		
$\delta(^{19}F)$	−62.1	−67.0	−60.7	−65.2				
$\delta(^{13}C)$ (*C*N)	127.5	172.3	n.o.	155.5	n.o.	n.o.	127.8	n.o.
$\delta(^{15}N)$	−103.0	−195.4	−161.0	−189.5	−181.9	−147.7	n.o.	n.o.
$\delta(^{31}P)$ *trans*			44.2	30.6	47.1	33.1	44.3	35.3
$\delta(^{31}P)$ *cis*			30.6	31.0	31.6	31.5	32.1	32.8
$^1J(^{13}CF_3,^{19}F)$	303.2	304.8	304.7	305.4				
$^nJ(^{15}N,^{31}P)$ *trans*[d]			38.2	8.8	37.8	6.7	n.o.	n.o.
$^nJ(^{15}N,^{31}P)$ *cis*[d]			4.7	1.6	5.1	n.o.	n.o.	n.o.
$^1J(^{31}P,^{103}Rh)$ *trans*			178.0	142.0	176.6	146.3	170	142.4
$^1J(^{31}P,^{103}Rh)$ *cis*			138.1	134.0	139.1	137.1	136	144.2
$^nJ(^{15}N,^{103}Rh)$[e]			17.9	n.o.	18.1	3.9	n.o.	n.o.
$^2J(^{31}P,^{31}P)$			41.0	39.5	40.9	38.4	39	37.5
$^4J(^{19}F,^{19}F)$	6.3	5.9	6.5	6.0				
$^1\Delta^{19}F(^{12/13}C)$	0.1315	0.1300	0.1323	0.1343				
solvent	CD_3CN	CD_3CN	CD_2Cl_2	CD_2Cl_2	$CDCl_3$	$CDCl_3$	CD_2Cl_2	$CDCl_3$
ref	*f*	*f*	*f*	*f*	5	5	10	4

[a] δ and Δ in ppm, J in Hz. [b] Anion: $[BF_4]^-$. [c] n.o. = not observed. [d] $n = 2$ or 3. [e] $n = 1$ or 2. [f] This work.

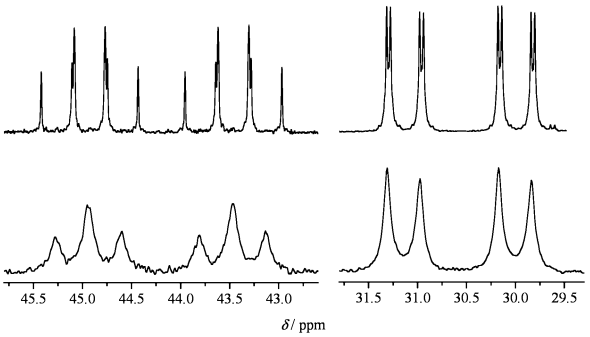

Figure 4. $^{31}P\{^1H\}$ NMR spectra of $(PPh_3)_3Rh^{15}NCB(CF_3)_3$ (upper trace) and $(PPh_3)_3Rh^{14}NCB(CF_3)_3$ (lower trace).

ppm with a relative intensity of two attributed to the *cis* P atoms. Both signals are split into doublets due to the coupling to the ^{103}Rh nucleus, and furthermore they exhibit couplings between the two nonequivalent ^{31}P nuclei. In the ^{15}N-labeled complex both signals are further split into doublets due to the interaction with ^{15}N. The chemical shifts and coupling constants are similar to those of the Ph_3BNC derivative (Table 4).[5]

Due to the small difference in $\delta(^{31}P)$ of the two different P nuclei ($\Delta = 0.4$ ppm) in $(PPh_3)_3RhCNB(CF_3)_3$ and in its ^{15}N isotopomer, the ^{31}P NMR spectra depicted in Figure 5 are of higher order. In addition the simulated spectra (*g*NMR)[21] are presented. The chemical shifts and coupling constants listed in Table 4 are derived from the simulations. $(PPh_3)_3RhCNB(CF_3)_3$ is the only example listed in Table 4 with $\delta(^{31}P)$ of the *cis* P nucleus being larger than $\delta(^{31}P)$ of the *trans* P nuclei; in general similar NMR spectroscopic data are reported for $(PPh_3)_3RhCNBPh_3$.[5]

While the ^{15}N resonance frequency of $(PPh_3)_3RhC^{15}NB(CF_3)_3$ (−189.5 ppm) is shifted to a higher value by 5.9 ppm than in the borate anion (−195.4 ppm), in the case of $(PPh_3)_3Rh^{15}NCB(CF_3)_3$ (−161.0 ppm) a shift of −58 ppm compared to the $[(CF_3)_3BC^{15}N]^-$ anion (−103.0 ppm) is found. In contrast to the ^{31}P chemical shifts, $\delta(^{15}N)$ of $(PPh_3)_3RhC^{15}NB(CF_3)_3$ and $(PPh_3)_3Rh^{15}NCB(CF_3)_3$ differ much more from those of the respective Ph_3B derivatives (Table 4). In the ^{15}N NMR spectrum of $(PPh_3)_3RhC^{15}NB(CF_3)_3$ a broad singlet is observed. The lack

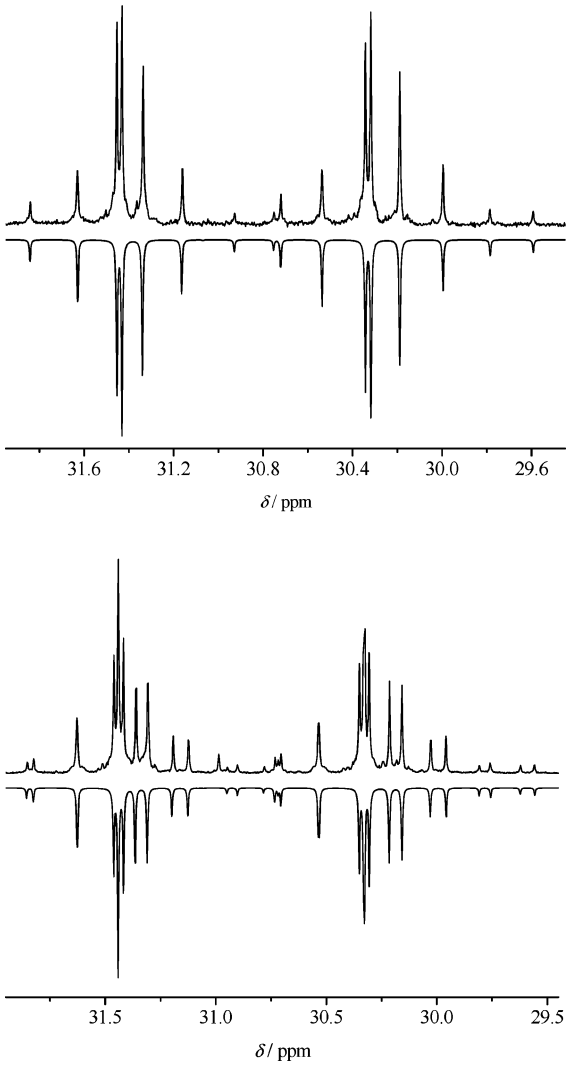

Figure 5. $^{31}P\{^1H\}$ NMR spectra of $(PPh_3)_3RhC^{14}NB(CF_3)_3$ (upper traces) and $(PPh_3)_3RhC^{15}NB(CF_3)_3$ (lower traces); simulated spectra (*g*NMR) inverted.

of any splittings is due to small coupling constants and to the line broadening caused by the interaction with the quadrupolar ^{11}B nucleus. The ^{15}N signal of $(PPh_3)_3Rh^{15}NCB(CF_3)_3$ in Figure 6 is split into a doublet ($^1J(^{15}N,^{103}Rh) = 17.9$ Hz) of doublets ($^2J(^{15}N,^{31}P) = 38.2$ Hz, *trans* P) of triplets ($^2J(^{15}N,^{31}P) = 4.7$

(19) Geoffroy, G. L.; Keeney, M. E. *Inorg. Chem.* **1977**, *16*, 205.
(20) Tolman, C. A.; Meakin, P. Z.; Lindner, D. L.; Jesson, J. P. *J. Am. Chem. Soc.* **1974**, *96*, 2762.
(21) Budzelaar, P. H. M. *g*NMR (V 4.1.0); Chem Research GmbH, 1995−1999.

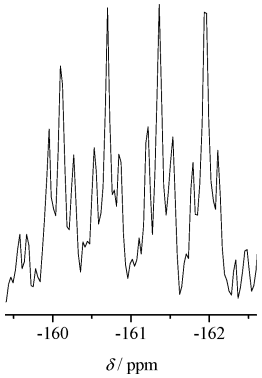

Figure 6. $^{15}N\{^{1}H\}$ NMR spectrum of $(PPh_3)_3Rh^{15}NCB(CF_3)_3$.

Hz, *cis* P). These values are close to those found for $(PPh_3)_3Rh^{15}NCBPh_3$ (Table 4).[5]

In the ^{11}B and ^{19}F NMR spectra of both Rh(I) complexes only broad singlets are observed, due to the quadrupolar moment of the ^{11}B nuclei. A dynamic effect, for example ligand exchange, as reason for the line broadening can be excluded because (i) no significant temperature dependence of the signal shape is observed, (ii) a similar line broadening was found for $(CF_3)_3BNCMe$[13] and $(CF_3)_3BCNMe$,[22] and (iii) in the $^{19}F\{^{11}B\}$ NMR spectra sharp signals are observed. The $^{1}J(^{13}CF_3,^{19}F)$ and $^{4}J(^{19}F,^{19}F)$ coupling constants as well as the $^{1}\Delta^{19}F(^{12/13}C)$ isotopic shifts derived from $^{19}F\{^{11}B\}$ experiments are listed in Table 4. There is nearly no difference in $\delta(^{11}B)$ and only a small change in $\delta(^{19}F)$ between the noncoordinated borate anions and $(PPh_3)_3RhCNB(CF_3)_3$ as well as $(PPh_3)_3RhNCB(CF_3)_3$, respectively (Table 4).

Summary and Conclusion

The first examples of transition metal complexes of $[(CF_3)_3BCN]^-$ and $[(CF_3)_3BNC]^-$ derived from reactions of $(PPh_3)_3RhCl$ with the potassium borates are presented. Their high thermal stabilities make them promising candidates for further chemistry and give a first insight into the application potential of $[(CF_3)_3BCN]^-$ and $[(CF_3)_3BNC]^-$ in coordination chemistry. The complexes are investigated by Raman, UV, and NMR spectroscopy, and their structures were determined by single-crystal X-ray diffraction.

A comparison of the CN stretching band positions and the structural parameters of $(PPh_3)_3RhCNB(CF_3)_3$ and $(PPh_3)_3RhNCB(CF_3)_3$ with those of $(PPh_3)_3RhCNBPh_3$ and $(PPh_3)_3RhNCBPh_3$[5,8] indicate that the tris(trifluoromethyl)borate ligands have a stronger *trans* effect and are stronger π-acceptors/weaker σ-donors. This trend is related to the higher Lewis acidity of $(CF_3)_3B$ in comparison with Ph_3B, in agreement with the data of $[(PPh_3)_3RhNCMe]^+$,[9,10] having the even stronger Lewis acid Me^+.

Experimental Section

General Considerations. Apparatus. The reactions involving air-sensitive compounds were performed under an Ar atmosphere using standard Schlenk line techniques. Solid materials were manipulated inside an inert atmosphere box (Braun, Munich, Germany) filled with argon, with a residual moisture content of less than 1 ppm.

$K[(CF_3)_3BNC]$ and $K[(CF_3)_3BCN]$ were synthesized as described previously.[11] $(PPh_3)_3RhCl$ was obtained from Strem Chemicals and used without further purification. All dry solvents were obtained from Aldrich and transferred under an Ar atmosphere into 1 L round-bottom flasks equipped with valves with PTFE stems (Young, London) and charged with molecular sieves (4 Å).

Single-Crystal X-ray Diffraction. Crystals of $(PPh_3)_3RhCNB(CF_3)_3$ and $(PPh_3)_3RhNCB(CF_3)_3\cdot1.5CH_2Cl_2$ suitable for X-ray diffraction were obtained by slow diffusion of pentane into dichloromethane solutions. Diffraction data were collected at 100 K on a KappaCCD diffractometer (Bruker AXS) using Mo Kα radiation ($\lambda = 0.71073$ Å) and either a graphite monochromator (for the isocyanide) or a focusing graded multilayer mirror (XENOCS). Frames were integrated using DENZO, and an empirical absorption correction (scalepack) was applied.[23] Crystal structures were determined using SHELXS-97,[24] and full-matrix least-squares refinements based on F^2 were performed using SHELXL-97.[25] Molecular structure diagrams were drawn using the program Diamond.[26] A summary of experimental details and crystal data is collected in Table 5. X-ray crystallographic files in CIF format have been deposited at the Cambridge Crystallographic Center under the deposition numbers CCDC-252111 for $(PPh_3)_3RhCNB(CF_3)_3$ and CCDC-252112 for $(PPh_3)_3RhNCB(CF_3)_3\cdot1.5CH_2Cl_2$. Copies of the data can be obtained free of charge on application to CCDC, 12 Union Road, Cambridge CB21EZ, UK (fax: (+44)1223-336-033; e-mail: deposit@ccdc.cam.ac.uk).

Raman Spectroscopy. Raman spectra were recorded on a Bruker RFS 100/S FT Raman spectrometer using the 1064 nm excitation (500 mW) of a Nd:YAG laser (DPY 301 II-N-OEM-500, Coherent, Lübeck, Germany).

UV Spectroscopy. The solids were dissolved in dry dichloromethane and transferred into a glass cell ($d = 5$ cm, $V = 20$ mL) equipped with quartz windows (Suprasil, Heraeus, Hanau) and a valve with a PTFE stem (Young, London). The UV spectra were recorded on a Perkin-Elmer Lambda 900 spectrometer in the range 200−700 nm.

NMR Spectroscopy. ^{1}H, ^{19}F, ^{31}P, and ^{11}B NMR spectra were recorded at room temperature on a Bruker Avance DRX-300 spectrometer operating at 300.13, 282.41, 121.49, or 96.29 MHz for ^{1}H, ^{19}F, ^{31}P, and ^{11}B nuclei, respectively. ^{13}C and ^{15}N NMR spectroscopic studies were performed at room temperature on a Bruker Avance DRX-500 spectrometer, operating at 125.758 or 50.678 MHz for ^{13}C and ^{15}N nuclei, respectively. The NMR signals were referenced to TMS (0.03% v/v) and $CFCl_3$ (0.1% v/v) as internal standards and 15% (v/v) $BF_3\cdot OEt_2$ in CD_3CN, 85% (v/v) H_3PO_4 in H_2O, and 10% (v/v) $MeNO_2$ in CD_3CN as external standards. Concentrations of the investigated samples were in the range 0.1−1 mol L^{-1}. The samples for NMR spectroscopic studies were prepared in 5 mm NMR tubes, equipped with special valves with PTFE stems (Young, London),[27] and dry CD_2Cl_2 was used as solvent. ^{31}P NMR spectra of $(PPh_3)_3RhC^{14}NB(CF_3)_3$ and $(PPh_3)_3RhC^{15}NB(CF_3)_3$ were simulated using the program *g*NMR.[21]

DSC Measurements. Thermoanalytical measurements were made with a Netzsch DSC204 instrument. Temperature and sensitivity calibrations in the temperature range 20−500 °C were carried out with naphthalene, benzoic acid, KNO_3, $AgNO_3$, $LiNO_3$, and CsCl. About 5−10 mg of the solid samples were weighed and contained in sealed aluminum crucibles. They were studied in the temperature range 20−600 °C with a heating rate of 5 K min^{-1}; throughout this process the furnace was flushed with dry nitrogen. For the evaluation of the output, the Netzsch Protens4.0 software was employed.

(22) Finze, M.; Bernhardt, E.; Willner, H.; Lehmann, C. W. *Inorg. Chem.* **2006**, *45*, 669.

(23) Otwinowski, Z.; Minor, W. *Methods Enzymol.* **1997**, *276*, 307.

(24) Sheldrick, G. M. *SHELXS-97*, Program for Crystal Structure Solution; University of Göttingen: Germany, 1997.

(25) Sheldrick, G. M. *SHELXL-97*, Program for Crystal Structure Refinement; University of Göttingen: Germany, 1997.

(26) *Diamond*-Visual Crystal Structure Information System, Ver. 2.1; Crystal Impact GbR, 1996−1999.

(27) Gombler, W.; Willner, H. *Int. Lab.* **1984**, 84.

Table 5. Crystallographic Data of $(PPh_3)_3RhCNB(CF_3)_3$ and $(PPh_3)_3RhNCB(CF_3)_3 \cdot 1.5CH_2Cl_2$

	$(PPh_3)_3RhCNB(CF_3)_3$	$(PPh_3)_3RhNCB(CF_3)_3 \cdot 1.5CH_2Cl_2$
empirical formula	$C_{58}H_{45}BF_9NP_3Rh$	$C_{59.5}H_{48}BCl_3F_9NP_3Rh$
fw [g mol^{-1}]	1133.58	1260.97
T [K]	100	100
color	orange	red-orange
cryst size [mm^3]	0.20 × 0.17 × 0.12	0.12 × 0.12 × 0.10
cryst syst, space group	monoclinic, $P2_1/n$ (no. 14)	monoclinic, $P2_1/c$ (no. 14)
unit cell dimens		
a [Å]	12.3421(1)	14.1585(1)
b [Å]	17.5818(2)	16.9086(2)
c [Å]	23.4382(2)	23.2446(2)
β [deg]	94.789(1)	94.045(1)
volume [Å^3]	5068.25(8)	5550.90(9)
Z	4	4
ρ_{calcd} [Mg m^{-3}]	1.486	1.509
absorp coeff [mm^{-1}]	0.505	0.609
F(000)	2304	2556
θ range [deg]	6.19−30.94	6.38−33.18
index ranges	$-17 \le h \le 17$, $-25 \le k \le 25$, $-29 \le l \le 33$	$-21 \le h \le 21$, $-25 \le k \le 26$, $-32 \le l \le 35$
no. of reflns collected/indep	71 780/15 896	107 004/20 922
no. of obsd reflns [$I > 2\sigma(I)$]	12495	14126
R(int) [%]	5.76	11.2
no. of data/restraints/params	15 896/0/6588	20 922/4/712
R_1 [$I > 2\sigma(I)$][a] [%]	3.7	6.0
wR_2 (all reflns)[b] [%]	13.4	15.0
goodness-of-fit on F^2 [c]	0.825	1.013
largest diff peak and hole [e Å^{-3}]	0.6 /−0.6	1.9 /−1.6

[a] $R_1 = (\sum||F_o| - |F_c||)/\sum|F_o|$. [b] $R_w = [\sum w(F_o^2 - F_c^2)^2/\sum w(F_o^2)^2]^{1/2}$, weighting scheme $w = [\sigma^2(F_o^2) + (aP)^2 + bP]^{-1}$. $P = (\max(0,F_o^2) + 2F_c^2)/3$. $(PPh_3)_3RhCNB(CF_3)_3$: $a = 0.1188$, $b = 0.0000$. $(PPh_3)_3RhNCB(CF_3)_3 \cdot 1.5CH_2Cl_2$: $a = 0.0568$, $b = 11.8616$. [c] Goodness-of-fit $S = \sum w(F_o^2 - F_c^2)^2/(m - n)$; m: no. of reflections, n: no. of variables.

$(PPh_3)_3RhNCB(CF_3)_3$. A 50 mL round-bottom flask equipped with a valve with a PTFE stem (Young, London), fitted with a PTFE-coated magnetic stirring bar, was charged with 72 mg (0.26 mmol) of $K[(CF_3)_3BCN]$ and 205 mg (0.22 mmol) of $(PPh_3)_3RhCl$. Then 20 mL of dry ethanol was condensed at −196 °C into the flask. The reaction mixture was warmed to room temperature and stirred for 3 days. During the reaction the solution became colorless and an orange solid precipitated. The solvent was removed under reduced pressure. In an argon atmosphere the residue was extracted twice with CH_2Cl_2 (40 and 20 mL), and the orange solution was separated from the residual colorless solid by filtration employing a glass frit. The solvent was removed in vacuo, and a solid was obtained. Yield: 227 mg (0.20 mmol, 91%). Anal. Calcd for $C_{58}H_{45}BF_9NP_3Rh$ (1133.63): C, 61.45; H, 4.00; N, 1.24. Found: C, 61.47; H, 4.02; N, 1.26.

$(PPh_3)_3RhCNB(CF_3)_3$. The synthesis of $(PPh_3)_3RhCNB(CF_3)_3$ was performed analogously to the preparation of its isomer $(PPh_3)_3RhNCB(CF_3)_3$. Yield: 147 mg (0.13 mmol, 86%). Anal. Calcd for $C_{58}H_{45}BF_9NP_3Rh$ (1133.63): C, 61.45; H, 4.00; N, 1.24. Found: C, 58.36; H, 3.07; N, 1.28. The poor agreement between calculated and found values is due to residual $K[(CF_3)_3BNC]$.

$(PPh_3)_3RhC^{15}NB(CF_3)_3$ and $(PPh_3)_3Rh^{15}NCB(CF_3)_3$. The ^{15}N-labeled compounds were prepared as described for the nonlabeled complexes from $K[(CF_3)_3B^{15}NC]$ and $K[(CF_3)_3BC^{15}N]$, respectively.

Acknowledgment. Financial support by the Deutsche Forschungsgemeinschaft, DFG, is acknowledged. Furthermore, we are grateful to Merck KGaA (Darmstadt, Germany) for providing chemicals used in this study. We thank Mr. M. Zähres (University Duisburg-Essen) for performing some NMR measurements and Mrs. R. Brülls (University Duisburg-Essen) for the elemental analyses.

Supporting Information Available: Files in cif format of the crystal data of $(PPh_3)_3RhCNB(CF_3)_3$ and $(PPh_3)_3RhNCB(CF_3)_3 \cdot 1.5CH_2Cl_2$ are available free of charge via the Internet at http://pubs.acs.org.

OM060135Z